Journal of Inorganic and Organometallic Polymers and Materials (2020) 30:400–409
https://doi.org/10.1007/s10904-019-01198-w

Eco-friendly Synthesis of Copper Oxide, Zinc Oxide and Copper Oxide–Zinc Oxide Nanocomposites, and Their Anticancer Applications

Elias E. Elemike[1] · Damian C. Onwudiwe[2,3] · Moganavelli Singh[4]

Received: 13 April 2019 / Accepted: 19 May 2019 / Published online: 23 May 2019

Abstract
Copper oxide nanoparticles (Cu_2O/CuO NPs), zinc oxide nanoparticles (ZnO NPs) and Cu_2O/CuO–ZnO nanocomposites have been prepared using *Alchornea cordifolia* leaf extract. The nanoparticles were synthesized using simple hydrothermal technique, followed by oven drying in the temperature range of 80–90 °C. The synthesis was monitored by UV–Vis spectroscopy, which confirmed the formation of the nanoparticles by showing peaks above 350 nm and a red shift was observed in the spectra of the nanocomposite. The structural evaluation of the nanomaterials using Fourier transform infra-red spectroscopy showed the presence of amides on their surface, indicative of their role as capping agents. The X-ray crystallographic studies showed mixed phase of Cu_2O/CuO NPs, and a hexagonal wurtzite phase for both the ZnO NPs and the nanocomposites. The elemental composition of the nanomaterials were explored using energy dispersive X-ray spectroscopy which confirmed the presence of the respective metals and oxygen; and a higher percentage of Zn (32.48%) compared to Cu (4.97%), in the nanocomposite. The average size of the nanoparticles in the composites were estimated at 3.54 nm with somewhat monodispersity, whereas the monometallic oxides gave agglomerated particles. The search for improved solution to cancerous growths necessitates the verification of the synthesized nanoparticles against cervical cancer using MTT assay method. In vitro cytotoxicity tests of the nanomaterials on cervical *Hela* cell lines showed efficacy in the order: Cu_2O/CuO–ZnO > ZnO NPs > Cu_2O/CuO NPs.

Keywords Semiconductors · Nanocomposites · Leaf extract · Photoluminescence · Anticancer

1 Introduction

The oxides of copper and zinc are among the benign metal oxides that have been reported to have biological applications. Nanoparticles have high surface area, and when integrated into one another, such as in nanocomposite, they give rise to materials with enlarged surface area which, in turn, exhibits extensive reactive sites, greater electron and mass transfer and enhanced efficacy [1]. Among many areas of significance reported for metal oxides such as in electronics, solar cells, photocatalysis, and sensing, biological applications is one of the interesting focus areas especially for the non-toxic nanoparticles.

The metal oxides have the ability of high production of reactive oxygen species (ROS) which are needed to curb the proliferation of cancer cells with high selectivity, but less sensitivity to normal cells [2]. Thus, it is important to evaluate their anticancer properties emanating from their varying sizes, shapes, and surface parameters which could be engineered by biosynthetic methods.

Nanobiotechnology has significantly impacted on medicine and pharmaceutical sciences in recent times, especially in drug design and delivery [3]. Hence, so many methods have been devised for the development of these

✉ Elias E. Elemike
chemphilips@yahoo.com

[1] Department of Chemistry, Federal University of Petroleum Resources, P.M.B. 1221 Effurun, Nigeria

[2] Material Science Innovation and Modelling (MaSIM) Research Focus Area, Faculty of Natural and Agricultural Science, North-West University (Mafikeng Campus), Private Bag X2046, Mmabatho, South Africa

[3] Department of Chemistry, Faculty of Natural and Agricultural Science, North-West University (Mafikeng Campus), Private Bag X2046, Mmabatho 2735, South Africa

[4] Non-viral Gene and Drug Delivery Laboratory, Department of Biochemistry, University of KwaZulu-Natal, Private Bag X54001, Durban 4000, South Africa

nanomaterials by manipulating their reaction conditions which influences their properties.

Due to the semiconducting properties of the nanometal oxides, the electrons in the valence band could gain energy and migrate from the topmost valence band to the lowest empty conduction band [4]. The movement of the electrons leaves positive holes behind in the valence band and creates reactive surfaces. The distance between these two surfaces is regarded as the band gap, and varies for different metal oxides. Apart from migration of electrons due to the absorption of energy, metal oxides nanoparticles also possess surface crystal defects which could induce the migration of electrons even without involving energy. Thus, when the electrons migrate to the conduction band, they could react with oxygen species to form superoxides and hydroxyl radicals which are effective in causing oxidative damage of DNA in cancer therapy [4].

Zinc oxide NPs is one of the non-toxic nanomaterials that could be used in biomedical applications. They have been used as antimicrobial and anticancer agents. In the treatment of HepG2 (liver cancer) and MCF-7 (breast cancer) cancer cells, the dosage of the nanoparticles was reported to determine the level of apoptosis and death of the cancer cell lines [5]. The interesting activity of ZnO NPs in cancer therapy may not only be attributed to their ability to generate ROS, but also on their unique electrostatic behaviour.

ZnO NPs have characteristic surface charges due to chemisorbed neutral hydroxyl groups. At high pH, protons (H^+) leave the surface making the nanoparticles to be negatively charged or producing partially bonded negative Zn–O surfaces [4]. At lower pH, the protonic environment causes the nanoparticles surfaces to be positively charged again. Under this condition, they could interact with the cancer cells since the tumour growth are primarily negatively charged phospholipids. The positive ZnO NPs—negative cancerous electrostatic interactions, therefore, causes phagocytosis and carcinoma cell toxicity.

Cancer is one of the ravaging diseases in present times, which affects both young and old due to lifestyle and poor feeding habits. There are many research centres around the world dedicated for cancer studies and possible ways of treatment. Cancer therapeutic treatment could be by the use of biological agents, alkylating agents, antimetabolites, nanomaterials etc. The most appealing of them all could be the use of nanomaterials, but the problem still remains whether the agents target the cancerous cells only or also affect other healthy cells leading to systemic toxicity.

The passive and active processes are two approaches of using nanomaterials in the treatment of cancerous tissues. In the passive method, the nanoparticles penetrate and diffuse so easily into the leaky cancerous tumour vasculature, thereby killing them. However, the inability to differentiate the tumour cells from the inflamed tissues becomes a challenge during the drug delivery. The active process could directly target the tumour cells alone and in such case the problem associated with the passive process is circumvented.

Novel chemotherapeutic agents involving the use of nanomaterials in slow and controlled release methods for cancer treatment have evolved with the advent of nanotechnology. In some of our investigations, we have reported plant mediated silver, gold, silver–gold bimetallic and gold–copper oxide nanoparticles as materials with cytotoxic potency against human cervical cancer [6–8]. Among all, the Ag–Au bimetallic nanoparticles synthesized using *Stigmaphyllon ovatum* leaf extract exhibited outstanding anticancer activities with the cytotoxicity increasing with increase in concentration of the nanoparticles. One of the reports also highlighted the toxic effects against H4IIE-luc and HuTu-80 at higher concentrations using Ag and Ag–Au bimetallic nanoparticles synthesized using *Solidago canadensis* extract [8].

Alchornea cordifolia (AC) plant belongs to the family of Euphorbiaceae, and it is mostly found in the West African coastal regions. This plant has been used traditionally as medicine to treat malaria, arthritis, systemic disorders in the intestine, respiratory and urinary tracts [9]. They have also been applied in eye treatment, wound healing and other skin infections. The stem, bark, roots and, more especially, the leaves have been applied for the listed purposes. Phytochemical screening of the plant leaf shows that it contains secondary metabolites such as phenolic compounds, steroids, tannins, alkaloids, flavonoids, xanthones etc. [10]. Okeke et al. have reported the broad spectrum antimicrobial activities of the unfractionated extract of the leaves due to synergistic potentiation from all the phytocomponents in the extract [11]. The leaves have also been reported to show less cytotoxic effect on some cancer cell lines [12].

In this work, copper sulphate and zinc acetate are used as precursors for the synthesis of their respective oxide, by employing the leaves extract of *A. cordifolia* as environmental friendly mediator. The aim is to develop cost effective metal oxides nanoparticles for possible cancer therapy.

2 Materials and Methods

Materials used: *Alchornea cordifolia* leaves, $Zn(CH_3COO)_2{\cdot}2H_2O$, $CuSO_4{\cdot}5H_2O$, *Hela* cells.

2.1 Preparation of the Leaf Extract

The leaves of *A. cordifolia* were air dried for 2–3 weeks, chopped and ground. The aqueous extract was made by heating a certain amount at a temperature of about 90 °C for 45 min. The solution was filtered and the filtrate used in the synthesis of the nanoparticles.

2.2 Preparation of Zinc Oxide Nanoparticles (ZnO NPs) Using AC Leaves Extract

The nanoparticles were prepared by using the green chemistry techniques in a hydrothermal synthetic procedure. Typically, 10 mM $Zn(CH_3COO)_2{\cdot}2H_2O$ was dissolved in water, and about 400 mL of the precursor solution was mixed with 80 mL of the leaf extract and 10 mL of 1 M of NaOH was added. The solution was stirred at 80–90 °C for 6 h. The formed colloidal solution was centrifuged and the nanoparticles were dried in an oven for 24 h at a temperature of 70–80 °C.

2.3 Preparation of Copper Oxide Nanoparticles (Cu_2O/CuO NPs) Using AC Leaves Extract

About 60 mL of the leaves extract was added to 300 mL of 2 mM $CuSO_4{\cdot}5H_2O$. The solution was stirred at a temperature of 80–90 °C for 4 h with a gradual addition of about 10 mL of 1 M NaOH. The dark green coloured colloidal solution obtained was centrifuged, washed and the nanoparticles dried in an oven for 24 h at temperature of about 80 °C.

2.4 Synthesis of Cu_2O/CuO–ZnO Nanocomposites

The Cu_2O/CuO–ZnO nanocomposite were synthesized firstly by mixing 400 mL of 10 mM $Zn(CH_3COO)_2{\cdot}2H_2O$ with 160 mL of the leaves extract and 10 mL of 1 M NaOH. It was heated with continuous stirring for about 4 h, after which 400 mL of 2 mM $CuSO_4{\cdot}5H_2O$ was added to the solution and heated at 80 °C for another 4 h. The solution was centrifuged, washed and the formed nanoparticles dried in an oven at 80 °C for 24–48 h.

2.5 Characterization of the Nanoparticles

The materials were characterised using different analytical instruments. The optical properties were studied using UV–Vis spectrophotometer and Perkin Elmer Lambda LS 55 photoluminescence spectrophotometer at excitation wavelength of 320 nm. The functional groups present in the leaves used as stabilizing agents was analysed using Bruker alpha-P Fourier Transform Infra-red (FTIR) spectrophotometer. The crystal phase and compositional analysis were carried out using powder X-ray diffractometer (XRD) (XPERT model, CuKα radiation, $\lambda = 1.5405$ Å at room temperature). The morphology and elemental composition of the nanoparticles were determined using FEI Quanta FEG 250 field emission gun microscope operating at 15 kV with the Energy dispersive X-ray (EDX) spectra obtained using Oxford Inca software. The particle sizes were analysed with the aid of JEOL2100 Transmission electron microscope (TEM) fitted with a LaB 6 electron gun at 5 kV, and the images were captured using a Gatan Ultrascan digital camera. For the sample preparation for TEM analysis, the samples were initially sonicated, dropped on a copper grids with a dropper and allowed to dry.

2.6 In Vitro Anticancer Studies of the Nanoparticles Using HeLa Cells

The cytotoxic effects of the nanoparticles on human cervical carcinoma (Hela) cells were carried out using standard procedures as reported in our earlier works [6, 7], using MTT assay method. The cells were cultured and seeded with different concentrations of the nanoparticles. The set up (cells containing nanoparticles) were incubated at 37 °C for 48 h in 5% CO_2 after which they were treated with MTT and further incubated at the same temperature for another 4 h. The product was dissolved in DMSO and absorbance were measured at wavelength of 570 nm in triplicate for consistency. Anticancer drug (5-fluorouracil), was used as standard, while untreated cell medium was used as control experiment.

3 Results and Discussion

3.1 Synthesis

The semiconductor nanoparticles of Cu_2O/CuO, ZnO and CuO–ZnO were synthesised using the leaf extract approach. During the synthesis, NaOH was used which enabled the required alkaline pH medium for the formation of the nanoparticles as indicated by the absorption peaks in the UV–Vis spectra of the samples. Under the same synthesis condition, the copper precursor and NaOH aided the formation of both cuprous and cupric oxide nanoparticles. The different colours of the colloidal solution were dirty green, white and milky white for the Cu_2O/CuO, ZnO and Cu_2O/CuO–ZnO nanoparticles respectively. After the synthesis, the nanoparticles were dried in an oven for about 24 h at < 100 °C, and the process was devoid of high temperature calcination process. Further characterisations of the nanoparticles were carried out using X-ray diffractometer, Energy dispersion X-ray spectrometer, scanning electron and transmission electron microscope.

3.2 UV–Vis Spectroscopic Studies of the Nanoparticles

UV–Vis spectroscopy is a non-destructive analytical technique for the analysis of nanoparticles. The wavelength of absorption, absorption peaks and intensities of the spectra depends on a lot of factors which may include the methods of preparation of the nanoparticles, surface effects, oxygen

vacancies, precursor types and concentration, particle size, morphology, impurity centres, pH, micro-strain and temperature [13].

The UV–Vis spectra of the nanoparticles gave different absorption peaks at 359, 369, and 373 nm for Cu_2O/CuO NPs, ZnO NPs and the CuO–ZnO nanocomposite respectively as shown in Fig. 1a–c.

The spectra of the Cu_2O/CuO–ZnO gave a broader peak, which may be due to the surface imperfection contributed by conjugation of two metal oxides [14]. Moreover, there was also a red shift in the absorption spectra when compared to the spectra of the monometallic oxides, CuO and ZnO, shown in Fig. 1a, b respectively. Yathisha et al. have also observed similar red shift in their reported Zn doped CuO nanocomposites [14]. In another related report by Gajendiran et al. they were of the opinion that absorption spectra of the nanoparticles tend to shift to longer wavelength (red shift) with an increase in the annealing temperature, which subsequently decreases the band gap energy [15]. The shift could be attributed to secondary electronic states formation influenced by the conjugate metal oxides together with electronic transitions between the valence and conduction band and secondly due to s, p–d spin exchange interaction which exist within the metal and oxygen atoms [14, 16, 17].

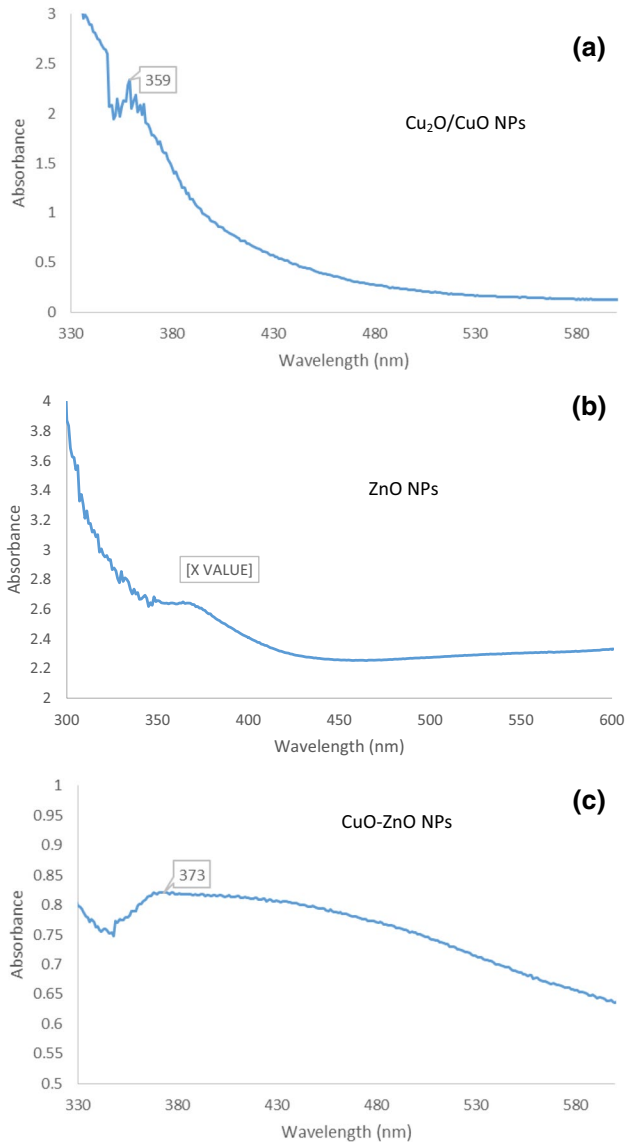

Fig. 1 UV–Vis spectra of **a** Cu_2O/CuO NPs, **b** ZnO NPs, **c** CuO–ZnO nanocomposite

3.3 Photoluminescence Spectra Studies of the Nanoparticles

The photoluminescence spectra gave important information on electronic energy transfer that occurs in semiconductor nanoparticles [18]. The various sizes and shapes of the nanoparticles, in addition to the excitation wavelength determine the emission peaks.

Figure 2 shows the photoluminescence spectra of the semiconductor nanoparticles. A strong emission peak appeared between 440 and 450 nm for the Cu_2O/CuO, ZnO and the CuO–ZnO nanoparticles at excitation wavelength of 320 nm. The luminescence intensity of the ZnO and CuO–ZnO peaks were higher than that of the copper oxide nanoparticles. The copper oxide NPs is a p-type semiconductor and the nature of the peaks exhibited may be due to the oxygen vacancies, surface effects, interstitial ion effect, electron recombination that existed between the donor and acceptor level defects of the nanoparticles. Moreover, the broad nature of the peak may arise from the co-appearance of the Cu_2O with CuO mixed crystal phases [19, 20]. Such broad nature of peaks have been attributed to CuO crystal defects and luminescence effects due to CuO/Cu_2O mixed crystalline phases [20].

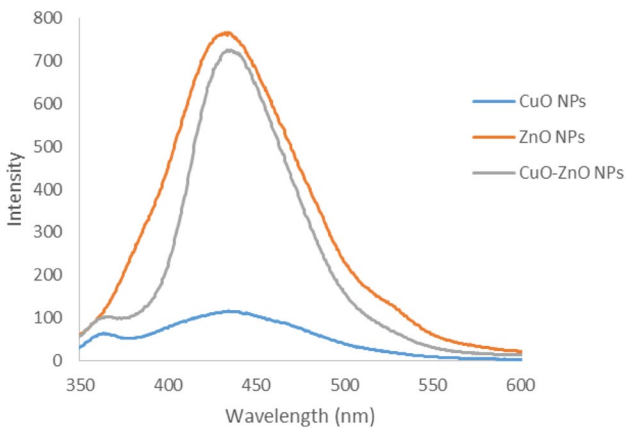

Fig. 2 Photoluminescence (PL) spectra of the nanoparticles at excitation wavelength of 320 nm

The ZnO NPs also showed emission peaks within the range of 440–450 nm with higher intensity compared to the copper oxide NPs. The nanoparticles were not annealed at higher temperature but rather dried over a long period of time in the oven below 100 °C in order to retain the components of the plant extracts which may have capped the nanoparticles. Therefore, the peaks observed may be due to low oxygen vacancies as annealing at high temperatures causes loss of oxygen and consequent creation of vacancies [21]. The emission peaks, however, may possibly be due to low temperature reaction conditions resulting into greater metal ion and surface oxygen interstitials [22].

The green region peaks in the range of 440–450 nm were also observed in the nanocomposites. The surface defects, metal and oxygen interstitial effects are responsible for such peaks and they act as electron–hole recombination centres. The intensity of the peak is lower than that of the pure ZnO NPs, but higher than the copper oxide NPs. The lowering of the intensity signified higher charge separation. The little decline in intensity observed in the nanocomposite compared to the ZnO NPs may be due to the lower percentage of the Cu compared to the ZnO. Therefore more concentrations of CuO in the nanocomposite could lead to further decrease in the peak intensity, profound p–n junction and increased charge separation [23].

3.4 FT-IR Studies

FTIR analysis was carried out on the leaf and the nanoparticles in order to ascertain the functional groups responsible for stabilization process.

Several absorption peaks were obtained from the leaves extract of the *A. cordifolia*. The peak around 3299 cm^{-1} indicated the presence of OH ascribed to biocomponents such as phenolic compounds. There were two strong peaks around 2909 and 2850 cm^{-1} which were due to C–H stretching vibrations either from the CH_2, or CH_3 of aliphatic compounds. The peak at 1730 cm^{-1} were that of carbonyl group, probably due to esters, ketones or aldehydes. Other absorption bands around 1612 cm^{-1}, 1455 cm^{-1} and 1010 cm^{-1} could be attributed to the bending vibrations of the OH, CH_3 and stretching vibration of the C–O bond respectively.

The nanoparticles exhibited absorption peaks similar to that of the leaves as shown in Table 1. The bands around 1548 cm^{-1}, 1566 cm^{-1} and 1564 cm^{-1} in all the nanoparticles could be attributed to functional groups due to secondary amide of proteins, which implied that the nanoparticles were possibly capped by such groups [24].

3.5 Powder X-ray Diffraction (pXRD) Compositional Analysis

The crystallinity, purity and compositional analysis of the nanoparticles were carried out using pXRD technique. The diffraction peaks displayed by the nanoparticles, as shown in Fig. 3, revealed the formation of the semiconductor nanoparticles. For Cu_2O/CuO nanoparticles, the 2θ peak values located at 35.97°, 38.45°, 48.42°, 61.35° represent (002), (111), (202), (113) crystal lattice orientation of monoclinic CuO (JCPDS 80-1268) respectively; whereas the 36.5°, 42.14°, 61.11°, 73.39° were assigned to the (111), (200), (220) and (311) orientations of the Cu_2O cubic phase respectively, similar to the diffraction patterns of JCPDS file no 05-0667 [25].

The (111) diffraction peak of the Cu_2O gave the most intense peak, which suggested that the crystals are dominated by (111) facets.

The formation of both Cu_2O and CuO phases may be due to inadequate concentration of NaOH [26]. More concentration of NaOH might possibly lead to the formation of only CuO phase. In addition, reports have shown that oxidation temperature below 300 °C also favours the formation of Cu_2O and higher oxidation temperature leads to formation of CuO [20].

The reaction mechanism could be proposed thus:

Firstly, copper hydroxide was formed from the copper salt and sodium hydroxide

$$CuSO_4 \cdot 5H_2O + NaOH \rightarrow Cu(OH)_2 + Na_2SO_4$$

Secondly, the formed $Cu(OH)_2$ then interacts with the biocomponents of the plant extracts such as flavonoids, phenolics, aldehydes etc. to form Cu_2O.

Table 1 Some absorption peaks and assigned functional groups of the plant leaf and synthesized nanoparticles

Functional groups	*Alchornea cordifolia* leaves (cm^{-1})	Cu_2O/CuO NPs (cm^{-1})	ZnO NPs (cm^{-1})	Cu_2O/CuO–ZnO NPs (cm^{-1})
OH	3299	–	–	–
C–H stretch	2909, 2850	–	–	–
C=O	1730	1692	1695	1690
O–H bend	1612	1548	1566	1564
CH_3 bend	1455	1420	1404	1415
C–O stretch	1010	1020	1017	1030

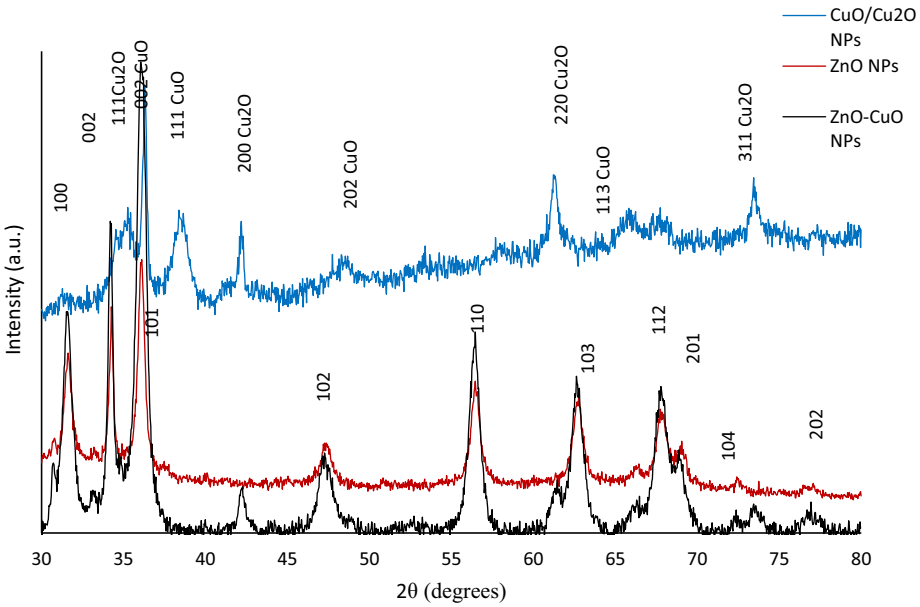

Fig. 3 Powder X-ray diffractograms of the synthesized nanoparticles

The addition of more OH^- would produce the more stable CuO as follows:

$$Cu(OH)_2 + xOH^- \rightarrow CuO + H_2O$$

The diffraction patterns displayed by the ZnO nanoparticles gave 2θ peaks at 31.78°, 34.32°, 36.52°, 47.36°, 56.21°, 62.49°, 67.63°, 68.25° corresponding to (100), (002), (101), (102), (110), (103), (112), (201) lattice indices attributed to ZnO hexagonal phase (JCPDS file: 36-1451) [27].

The nanocomposite gave peaks that reflects proper integration of both ZnO, CuO and Cu_2O nanoparticles in a wurtzite-like phase. It has been reported that composites with < 15% Cu shows one-phase wurtzite-like $Cu_xZn_{1-x}O$, whereas the ones with higher Cu content exhibits tenorite-like oxide ($Zn_xCu_{1-x}O$) phase [1]. Comparing the obtained diffraction peaks of the ZnO nanoparticles with the nanocomposites, the increased peak intensity of the nanocomposite signified enhanced crystallinity.

3.6 Morphological Studies

SEM and EDX were used to determine both the morphologies and compositions of the nanoparticles as shown in Fig. 4a–f. The micrographs showed spherical structures, which agglomerated into somewhat star-like nanostructures in the case of the CuO–ZnO nanocomposite.

The EDX showed elemental distribution of the nanoparticles as shown in the spectra and presented in Table 2. The ZnO nanoparticles gave peaks of Zn and O, while the CuO NPs showed peaks of Cu, O and S. The nanocomposite depicted the presence of all the three elements with higher percentage of Zn than Cu and the highest percentage of O as shown in Table 2.

3.7 TEM Analysis/Particle Size Determination

The size and shape of the nanoparticles are key to their applications, which makes the microscopic investigation an important technique in nanotechnology. The TEM images of the NPs showed agglomerated spherically shaped particles with average size of 75.22 nm; mixed nanospheres and nanoblocks of clustered CuO NPs with average size of 16.25 nm, and quantum dots of 3.54 nm size for the CuO–ZnO nanocomposites as shown in Fig. 5a–c.

The ZnO and Cu_2O/CuO NPs were polydispersed showing variability in the particle size while the ZnO–CuO NPs were monodispersed. The nature of the nanoparticles obtained here are similar to earlier reports [28]. The nanoparticles were not subjected to high temperature annealing, but were oven dried at long hours below 100 °C to retain the capping effect of the plant biomolecules. Such procedure is energy saving, but might have led to the agglomerated nature of the CuO and ZnO NPs. On the other hand, the uniform quantum size obtained for the nanocomposites is very interesting and may have occurred due to lower concentration influence of the copper and the procedure employed in the nanocomposite synthesis.

3.8 In Vitro Cytotoxicity Behaviour of the Nanoparticles Towards *Hela* Cell Lines

The in vitro cytotoxicity of the Cu_2O/CuO, ZnO NPs and Cu_2O/CuO–ZnO NPs against the *Hela* cells was verified using MTT assay method and the results were compared to a standard anticancer drug, 5-fluorouracil. Different concentrations of 20, 40, 60, 80, and 100 µg/µL were prepared for the nanoparticles, standard drug and control and were used

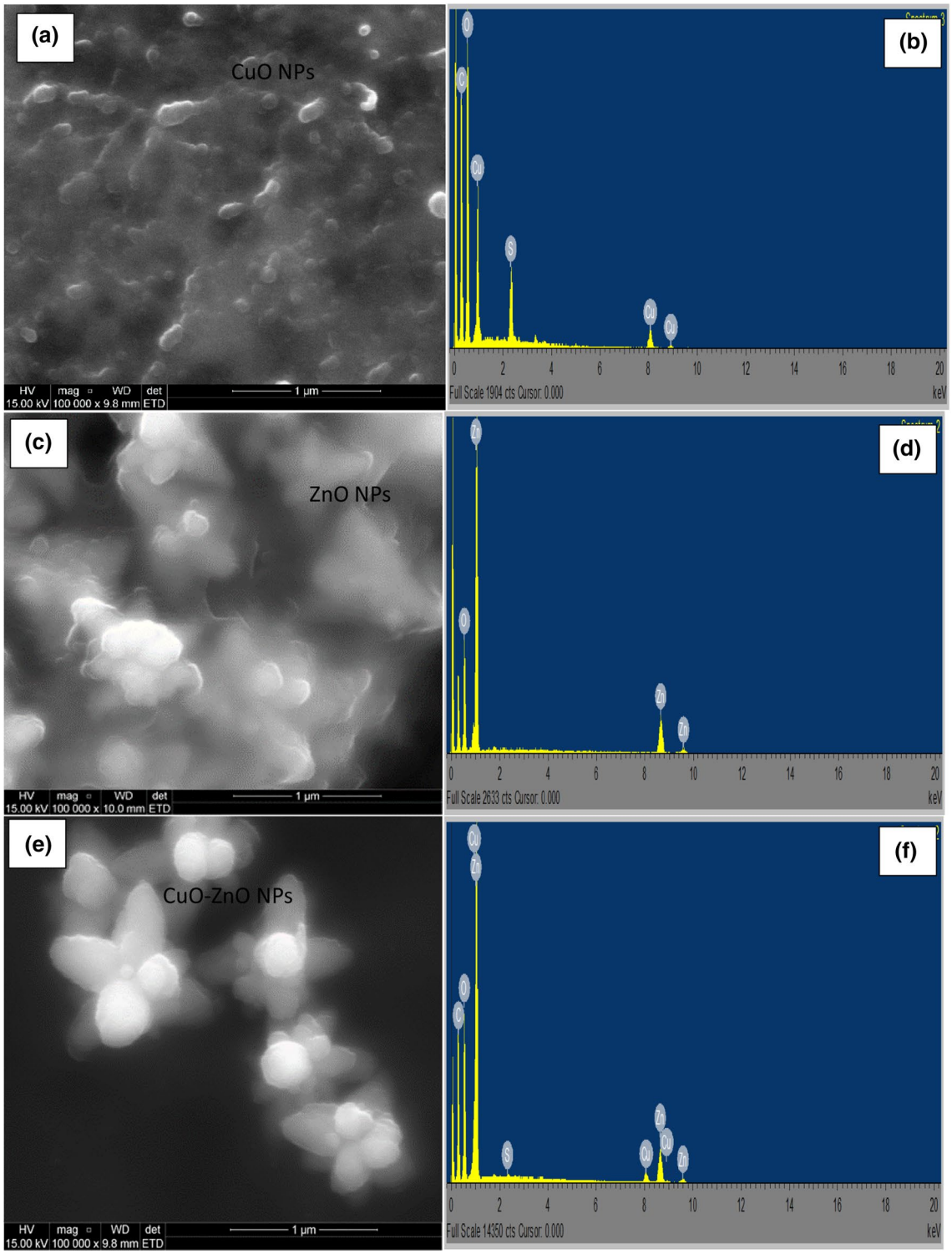

Fig. 4 SEM images (**a**, **c**, **e**), and the corresponding EDX spectra (**b**, **d**, **f**) of the synthesized nanoparticles

for the studies. The experiments were repeated three times for consistency and the average values recorded as shown in Table 3. The results obtained showed that the cells viability reduced as concentration of the nanoparticles increased. All the nanoparticles synthesized exhibited cytotoxic potency against the Hela cells with the Cu_2O/CuO–ZnO nanocomposites showing the highest activity. ZnO NPs showed higher anticancer potency than the CuO NPs. However,

Table 2 Compositional analysis of the nanoparticles using EDXS

Sample	Cu	Zn	O	S
CuO	38.01	–	52.55	9.44
ZnO	–	36.63	63.37	–
CuO-ZnO	4.97	32.48	62.14	0.41

they were not as effective as the standard drug. Compared to Au–Ag bimetallic and Au–CuO nanoparticles in our previous investigations, the present work demonstrated lower efficiency. In addition, the bimetallic or metal–metal oxide nanocomposites appear to be more effective than the monometallic counterparts.

The work of Dobrucka et al. has shown that Au–CuO and CuO–ZnO nanoparticles prepared from *Cnici benedicti* leaf extract inhibited the viability of rat glioma C6 cells

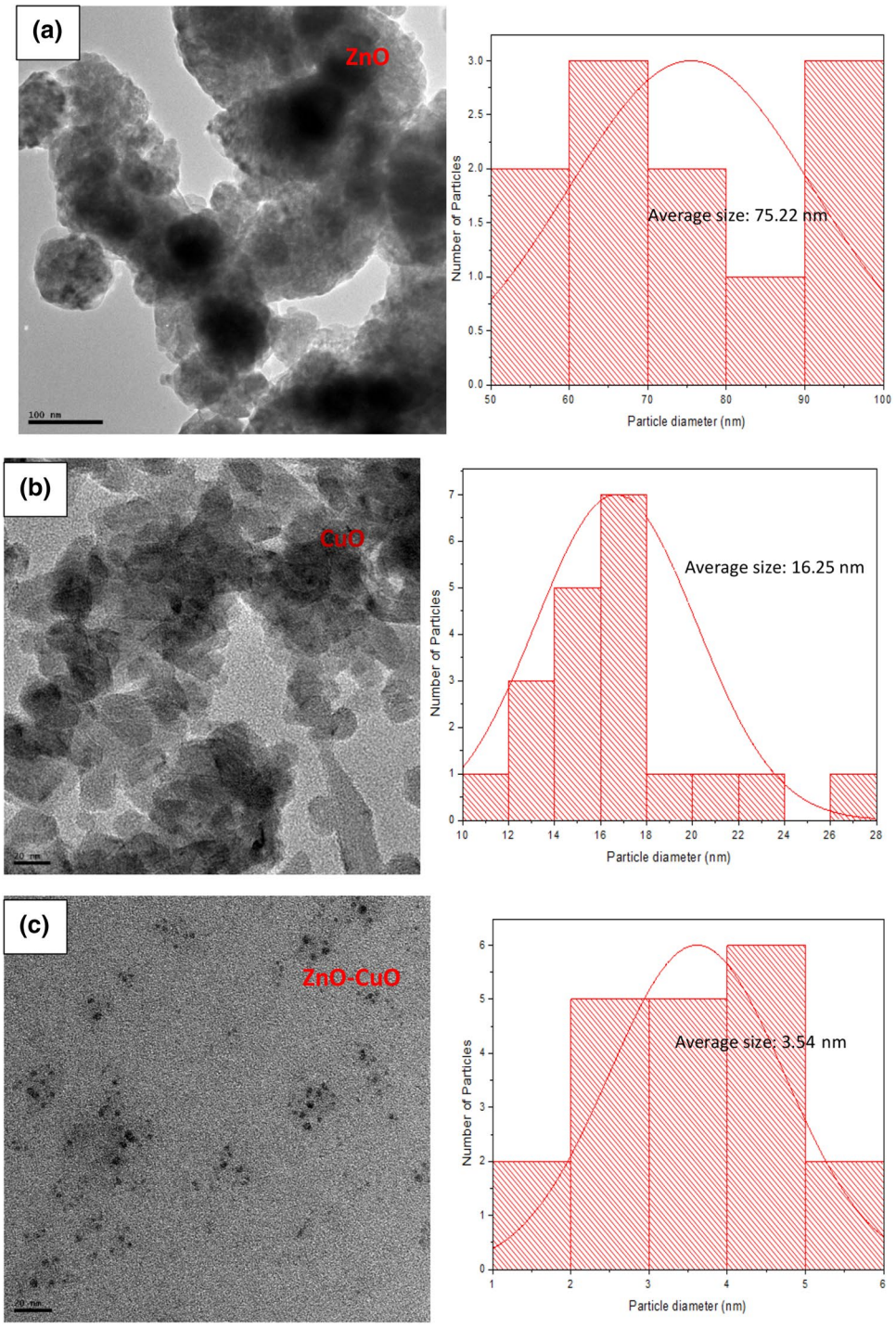

Fig. 5 TEM images of **a** ZnO NPs, **b** CuO NPs and **c** ZnO–CuO nanoparticles, and their corresponding particle size distribution

Table 3 In vitro cytotoxicity results using *Hela* cell lines at different nanoparticles concentration

Nanoparticles (NPs)	20 µg/mL	40 µg/mL	60 µg/mL	80 µg/mL	100 µg/mL
Cell only	100 ± 0.71	100 ± 0.71	100 ± 0.71	100 ± 0.71	100 ± 0.71
5-Fluorouracil	82.39 ± 0.86	58.36 ± 2.79	48.87 ± 1.25	42.98 ± 1.28	29.74 ± 5.89
CuO NPs	67.74 ± 6.78	64.68 ± 6.23	65.40 ± 0.93	66.90 ± 4.03	63.64 ± 8.34
ZnO NPs	63.93 ± 12.20	53.51 ± 2.31	50.97 ± 8.60	44.76 ± 9.21	44.05 ± 0.91
ZnO–CuO NPs	56.30 ± 6.38	56.44 ± 4.28	58.17 ± 10.54	40.52 ± 0.27	39.94 ± 5.01

according to the administered dose and exposure time [29]. The Au–CuO showed improved cytotoxicity more than the CuO–ZnO nanoparticles. This further shows that the noble metal bimetallic nanoparticles and the noble metals–metal oxides composites are more effective anticancer agents that the composites of two or more metal oxides.

Nagajyothi et al. have reported that CuO NPs can efficiently reduce the proliferation of *Hela* cells by apoptosis [30]. In another similar report by Rehana et al. plant extract mediated CuO NPs showed more cytotoxic activity towards some carcinoma cells (MCF-7, HeLa, Hep-2, A549) than the chemical synthesized ones [24]. Further studies also showed that the nanoparticles were not toxic to the normal human dermal fibroblast (NHDF) cells.

On the other hand, Moon et al. have reported selective toxicity of ZnO chips through Zn^{2+} release towards human B lymphocyte *Raji* cells without harming the peripheral blood mononuclear cells [31]. ZnO nanoparticles are biocompatible and biosafe nanomaterials at concentrations lower than 100 mg/mL irrespective of their shape, but this assertion does not circumvent the proper verification of ZnO NPs selective apoptosis in carcinoma cells before clinical applications [31, 32].

During proliferation of cancerous cells, there is a constant chain growth of radicals or electrons which are continuously transported [33]. The mechanism of the apoptosis of the carcinoma cells by the nanoparticles occurs through generation of ROS and subsequent destruction of transport pathway of the electrons.

Since ZnO and CuO NPs are effective in cancer therapy, the nanocomposite is expected to be better, and this has been shown by this study. However, there are still un-filled gaps on such nanocomposites and this necessitates further studies.

4 Conclusion

The development in nanotechnology has prompted the use of benign materials to offer chemotherapeutic solutions towards proliferation of tumor cells.

Copper and zinc oxide nanoparticles are eco-friendly metal oxides that may produce reactive oxygen species capable of hampering the multiplication of tumor cells by mechanism of apoptosis.

The optical studies of the *A. cordifolia* mediated nanoparticles showed absorption peaks around 359, 369, and 373 nm for Cu_2O/CuO NPs, ZnO NPs and Cu_2O/CuO–ZnO NPs respectively. Further photoluminescence spectroscopy revealed peaks in the green region around 440–450 nm in all the nanoparticles, and the low percentage of the copper in the nanocomposites decreased the intensity of the luminescence peak. The average sizes of the nanoparticles were obtained from the TEM images as 75.22, 16.25 and 3.54 nm for ZnO NPs, Cu_2O/CuO NPs and the CuO–ZnO nanocomposite. The images also revealed agglomeration on the monometallic oxides, but well dispersed uniform quantum dots for the nanocomposites. These nanoparticles showed good anticancer properties with the cell viability decreasing as the concentration of the nanoparticles increased. The Cu_2O/CuO–ZnO nanocomposites displayed the best results among the three compounds tested, followed by the ZnO NPs. The Cu_2O/CuO NPs portrayed the least cytotoxic effect on the *Hela* cells, but all the nanoparticles were not as effective as the standard 5-fluorouracil drug. Nevertheless, the potency of the nanomaterials could be improved through their formational and structural dynamics.

Acknowledgements The authors wish to acknowledge Dr Innocent Shuro of the Laboratory for Electron Microscopy CRB, NWU, for the microscopy analysis and Dr Remy for the powder X-ray crystallography. The management of North West University South Africa and Federal University of Petroleum Resources Effurun, Nigeria are also acknowledged for the enabled platform for the success of this work.

Compliance with Ethical Standards

Conflict of interest The authors declare no conflict of interest.

References

1. S. Das, V.C. Srivastava, An overview of the synthesis of CuO-ZnO nanocomposite for environmental and other applications. Nanotechnol. Rev. **7**, 267–282 (2018). https://doi.org/10.1515/ntrev-2017-0144
2. R. Yuan, H. Xu, X. Liu, Y. Tian, C. Li, X. Chen, S. Su, I. Perelshtein, A. Gedanken, X. Lin, Zinc-doped copper oxide nanocomposites inhibit the growth of human cancer cells through reactive oxygen species-mediated NF-κB activations. ACS Appl. Mater. Interfaces **8**, 31806–31812 (2016). https://doi.org/10.1021/acsami.6b09542

3. E.G. Halevas, A.A. Pantazaki, Copper nanoparticles as therapeutic anticancer agents. Nanomed. Nanotechnol. J. **2**, 119 (2018)
4. P.K. Mishra, H. Mishra, A. Ekielski, S. Talegaonkar, B. Vaidya, Zinc oxide nanoparticles: a promising nanomaterial for biomedical applications. Drug Discov. Today **22**, 1825–1834 (2017). https://doi.org/10.1016/j.drudis.2017.08.006
5. M. Vinardell, M. Mitjans, Antitumor activities of metal oxide nanoparticles. Nanomaterials **5**, 1004–1021 (2015). https://doi.org/10.3390/nano5021004
6. E.E. Elemike, D.C. Onwudiwe, N. Nundkumar, M. Singh, O. Iyekowa, Green synthesis of Ag, Au and Ag-Au bimetallic nanoparticles using *Stigmaphyllon ovatum* leaf extract and their in vitro anticancer potential. Mater. Lett. **243**, 148–152 (2019). https://doi.org/10.1016/j.matlet.2019.02.049
7. E.E. Elemike, D.C. Onwudiwe, N. Nundkumar, M. Singh, CuO and Au-CuO nanoparticles mediated by *Stigmaphyllon ovatum* leaf extract and their anticancer potential. Inorg. Chem. Commun. (2019). https://doi.org/10.1016/j.inoche.2019.03.039
8. T.L. Botha, E.E. Elemike, S. Horn, D.C. Onwudiwe, J.P. Giesy, V. Wepener, Cytotoxicity of Ag, Au and Ag-Au bimetallic nanoparticles prepared using golden rod (*Solidago canadensis*) plant extract. Sci. Rep. **9**, 1–8 (2019). https://doi.org/10.1038/s41598-019-40816-y
9. C.V. Simoben, F. Ntie-Kang, L.L. Lifongo, S.B. Babiaka, W. Sippl, L.M. Mbaze, The uniqueness and therapeutic value of natural products from West African medicinal plants, part III: least abundant compound classes. RSC Adv. **4**, 40095–40110 (2014). https://doi.org/10.1039/C4RA05376A
10. T. Walker, E. Essien, W. Setzer, J. Newby, O. Ekundayo, Characterization and antimicrobial activity of volatile constituents from fresh fruits of *Alchornea cordifolia* and *Canthium subcordatum*. Medicines **3**, 1 (2015). https://doi.org/10.3390/medicines3010001
11. I.N. Okeke, A.O. Ogundaini, F.O. Ogungbamila, A. Lamikanra, Antimicrobial spectrum of *Alchornea cordifolia* leaf extract. Phyther. Res. **13**, 67–69 (1999). https://doi.org/10.1002/(SICI)1099-1573(199902)13:1%3c67:AID-PTR366%3e3.0.CO;2-F
12. X.S. Noundou, Isolation and identification of anticancer compounds from Alchornea species and their encapsulation into nanostructured drug delivery systems. University of Johannesburg, 2012
13. E.E. Elemike, D.C. Onwudiwe, O. Arijeh, H.U. Nwankwo, Plant-mediated biosynthesis of silver nanoparticles by leaf extracts of *Lasienthra africanum* and a study of the influence of kinetic parameters. Bull. Mater. Sci. **40**, 129–137 (2017). https://doi.org/10.1007/s12034-017-1362-8
14. R.O. Yathisha, Y. Arthoba Nayaka, P. Manjunatha, H.T. Purushothama, M.M. Vinay, K.V. Basavarajappa, Study on the effect of Zn^{2+} doping on optical and electrical properties of CuO nanoparticles. Physica E **108**, 257–268 (2019). https://doi.org/10.1016/j.physe.2018.12.021
15. T.K.J. Gajendiran, C. Ramamoorthy, K.C. Prabhu Sankar, T. Rajkumar Sam Kingsly, V. Kamalakannan, Optical and luminescent properties of NiO-CuO nanocomposite by the precipitation method. J. Adv. Chem. Sci. **2**, 223–226 (2016)
16. M. Ashokkumar, S. Muthukumaran, Tuning of energy gap, microstructure, optical and structural properties of Cr doped $Zn_{0.96}Cu_{0.04}O$ nanoparticles. Powder Technol. **258**, 157–164 (2014). https://doi.org/10.1016/j.powtec.2014.03.013
17. Ü. Özgür, Y.I. Alivov, C. Liu, A. Teke, M.A. Reshchikov, S. Doğan, V. Avrutin, S.-J. Cho, H. Morkoç, A comprehensive review of ZnO materials and devices. J. Appl. Phys. **98**, 041301 (2005). https://doi.org/10.1063/1.1992666
18. S. Dagher, Y. Haik, A.I. Ayesh, N. Tit, Synthesis and optical properties of colloidal CuO nanoparticles. J. Lumin. **151**, 149–154 (2014). https://doi.org/10.1016/j.jlumin.2014.02.015
19. X. Zhao, P. Wang, Z. Yan, N. Ren, Room temperature photoluminescence properties of CuO nanowire arrays. Opt. Mater. (Amst) **42**, 544–547 (2015). https://doi.org/10.1016/j.optmat.2014.12.032
20. C.Y. Huang, A. Chatterjee, S.B. Liu, S.Y. Wu, C.L. Cheng, Photoluminescence properties of a single tapered CuO nanowire. Appl. Surf. Sci. **256**, 3688–3692 (2010). https://doi.org/10.1016/j.apsusc.2010.01.007
21. S. Venkataprasad Bhat, S.R.C. Vivekchand, A. Govindaraj, C.N.R. Rao, Photoluminescence and photoconducting properties of ZnO nanoparticles. Solid State Commun. **149**, 510–514 (2009). https://doi.org/10.1016/j.ssc.2009.01.014
22. R. Yatskiv, J. Grym, Luminescence properties of hydrothermally grown ZnO nanorods. Superlattices Microstruct. **99**, 214–220 (2016). https://doi.org/10.1016/j.spmi.2016.02.021
23. D. Han, B. Li, S. Yang, X. Wang, W. Gao, Z. Si, Q. Zuo, Y. Li, Y. Li, Q. Duan, D. Wang, Engineering charge transfer characteristics in hierarchical Cu2S QDs @ ZnO nanoneedles with p–n heterojunctions: towards highly efficient and recyclable photocatalysts. Nanomaterials **9**, 16 (2018). https://doi.org/10.3390/nano9010016
24. D. Rehana, D. Mahendiran, R.S. Kumar, A.K. Rahiman, Evaluation of antioxidant and anticancer activity of copper oxide nanoparticles synthesized using medicinally important plant extracts. Biomed. Pharmacother. **89**, 1067–1077 (2017). https://doi.org/10.1016/j.biopha.2017.02.101
25. L. Xiong, H. Yu, C. Nie, Y. Xiao, Q. Zeng, G. Wang, B. Wang, H. Lv, Q. Li, S. Chen, Size-controlled synthesis of Cu_2O nanoparticles: size effect on antibacterial activity and application as a photocatalyst for highly efficient H_2O_2 evolution. RSC Adv. **7**, 51822–51830 (2017). https://doi.org/10.1039/c7ra10605j
26. N. Zayyoun, L. Bahmad, L. Laânab, B. Jaber, The effect of pH on the synthesis of stable Cu_2O/CuO nanoparticles by sol–gel method in a glycolic medium. Appl. Phys. A **122**, 3–8 (2016). https://doi.org/10.1007/s00339-016-0024-9
27. P. Jamdagni, P. Khatri, J.S. Rana, Green synthesis of zinc oxide nanoparticles using flower extract of *Nyctanthes arbor-tristis* and their antifungal activity. J. King Saud Univ.—Sci. **30**, 168–175 (2018). https://doi.org/10.1016/j.jksus.2016.10.002
28. M. Ponnar, C. Thangamani, P. Monisha, S.S. Gomathi, K. Pushpanathan, Influence of Ce doping on CuO nanoparticles synthesized by microwave irradiation method. Appl. Surf. Sci. **449**, 132–143 (2018). https://doi.org/10.1016/j.apsusc.2018.01.126
29. R. Dobrucka, M. Kaczmarek, M. Łagiedo, A. Kielan, J. Długaszewska, Evaluation of biologically synthesized Au-CuO and CuO-ZnO nanoparticles against glioma cells and microorganisms. Saudi Pharm. J. **27**, 373–383 (2019). https://doi.org/10.1016/j.jsps.2018.12.006
30. P.C. Nagajyothi, P. Muthuraman, T.V.M. Sreekanth, D.H. Kim, J. Shim, Green synthesis: in vitro anticancer activity of copper oxide nanoparticles against human cervical carcinoma cells. Arab. J. Chem. **10**, 215–225 (2017). https://doi.org/10.1016/j.arabjc.2016.01.011
31. S.H. Moon, W.J. Choi, S.W. Choi, E.H. Kim, J. Kim, J.O. Lee, S.H. Kim, Anti-cancer activity of ZnO chips by sustained zinc ion release. Toxicol. Rep. **3**, 430–438 (2016). https://doi.org/10.1016/j.toxrep.2016.03.008
32. P. Sivakumar, M. Lee, Y.S. Kim, M.S. Shim, Photo-triggered antibacterial and anticancer activities of zinc oxide nanoparticles. J. Mater. Chem. B. **6**, 4852–4871 (2018). https://doi.org/10.1039/c8tb00948a
33. J. Jiang, J. Pi, J. Cai, The advancing of zinc oxide nanoparticles for biomedical applications. Bioinorg. Chem. Appl. **2018**, 1–18 (2018). https://doi.org/10.1155/2018/1062562